SOIL Discuss., 2, 1103–1133, 2015
www.soil-discuss.net/2/1103/2015/
doi:10.5194/soild-2-1103-2015

SOIL
Discussions
Open Access

Characterization of stony soils' hydraulic conductivity using laboratory and numerical experiments

M. Pichault[1], **E. Beckers**[1], **A. Degré**[1], **and S. Garré**[1,2]

[1]Université de Liège, Gembloux Agro-Bio Tech, Department of Biosystems Engineering, Passage des déportés 2, 5030 Gembloux, Belgium
[2]Université de Liège, Gembloux Agro-Bio Tech, AgricultureIsLife.be, Passage des déportés 2, 5030 Gembloux, Belgium

Received: 13 October 2015 – Accepted: 19 October 2015 – Published: 29 October 2015

Correspondence to: S. Garré (sarah.garre@ulg.ac.be)

Published by Copernicus Publications on behalf of the European Geosciences Union.

Abstract

Determining soil hydraulic properties is of major concern in various fields of study. Though stony soils are widespread across the globe, most studies deal with gravel-free soils so that the literature describing the impact of stones on soil's hydraulic conductivity is still rather scarce. Most frequently, models characterizing the saturated hydraulic conductivity of stony soils assume that the only effect of rock fragments is to reduce the volume available for water flow and therefore they predict a decrease in hydraulic conductivity with an increasing stoniness. The objective of this study is to assess the effect of rock fragments on the saturated and unsaturated hydraulic conductivity. This was done by means of laboratory and numerical experiments involving different amounts and types of coarse fragments. We compared our results with values predicted by the aforementioned models. Our study suggests that considering that stones only reduce the volume available for water flow might be ill-founded. We pointed out several drivers of the saturated hydraulic conductivity of stony soils, not considered by these models. On the one hand, the shape and the size of inclusions may substantially affect the hydraulic conductivity. On the other hand, the presence of rock fragments can counteract and even overcome the effect of a reduced volume in some cases. We attribute this to the creation of voids at the fine earth-stone interface. Nevertheless, these differences are mainly important near to saturation. However, we come up with a more nuanced view regarding the validity of the models under unsaturated conditions. Indeed, under unsaturated conditions, the models seem to represent the hydraulic behaviour of stones reasonably well.

1 Introduction

Determining soil hydraulic properties is of primary importance in various fields of study such as soil physics, hydrology, ecology and agronomy. Information on hydraulic properties is essential to model infiltration and runoff, to quantify groundwater recharge, to simulate the movement of water and pollutants in the vadose zone, etc. (Bouwer and Rice, 1984). Most unsaturated flow studies only characterize the hydraulic properties of the fine fraction (particles smaller than 2 mm of diameter) of supposedly uniform soils (Bouwer and Rice, 1984; Buchter et al., 1994; Gusev and Novák, 2007). Nevertheless, in reality soils are heterogeneous media and may contain coarse inclusions (stones) of various sizes and shapes.

Stony soils are widespread across the globe (Ma and Shao, 2008) and represent a significant part of the agricultural land (Miller and Guthrie, 1984). Furthermore, their usage tend to increase because of erosion and cultivation of marginal lands (García-Ruiz, 2010). Yet little attention has been paid to the effects of the coarser fraction, so that the literature describing the impact of stones on soil hydraulic characteristics is still rather scarce (Ma and Shao, 2008; Novák and Šurda, 2010; Poesen and Lavee, 1994).

Many authors consider that the reduction of volume available for water flow is the only effect of stones on hydraulic conductivity. This hypothesis has led to formulas linking the hydraulic conductivity of the fine earth to those of the stony soils. They predict a decrease in effective saturated hydraulic conductivity (K_{se}) with an increasing volumetric stoniness (R_v) (Bouwer and Rice, 1984; Brakensiek et al., 1986; Hlaváčiková and Novák, 2014; Novák and Kňava, 2011; Peck and Watson, 1979; Ravina and Magier, 1984).

However, a number of studies do not observe this simple indirect relationship between the hydraulic conductivity and the stoniness (Beibei et al., 2009; Ma et al., 2010; Russo, 1983; Sauer and Logsdon, 2002). Russo (1983) conducted some in situ measurements of the K_{se} in soils containing a large amount of stones ($R_v > 35\,\%$) and, even if the K_{se} decreases with the stone content, he measured higher values of conductivity than expected based on the aforementioned models. In another study by Beibei et al. (2009), permeameter tests over samples of different gravimetric rock content (R_w) reveal that the K_{se} initially decreases at low R_w to a minimum value at $R_w = 40\,\%$ and then tends to increase to higher R_w. Laboratory tests conducted by Ma et al. (2010) showed the same overall behaviour, and found in addition a greater K_{se} at $R_v = 8\,\%$

than the one of the fine earth alone. Sauer and Logsdon (2002) also came up with surprising results while carrying out in situ infiltration tests. In saturated conditions, they measured higher hydraulic conductivity with increasing rock fragment content. However, with increasing negative pressure head (and particularly at $h = -12\,\mathrm{cm}$), they measured decreasing hydraulic properties with increasing rock fragment content. These controversial results suggest that other factors may play a substantial role in specific situations (Ma et al., 2010).

Indeed, ambivalent phenomena can intervene simultaneously, which makes the understanding of the effective hydraulic properties of stony soils very difficult. The reduced volume available for flow might be partially compensated by others factors. One contradictory effect might be, as pointed out by Ravina and Magier (1984), the creation of large pores in the rock fragments' vicinity. These authors directly observed large voids by cutting across a soil sample after its compaction, presumably due to translational displacement of densely packed fragments. This is in agreement with the observed increasing conductivity with increasing R_v. Indeed, the creation of new voids at the stone-fine earth interface can generate preferential flows and hence increase the effective hydraulic conductivity (Beibei et al., 2009; Cousin et al., 2003; Ravina and Magier, 1984; Sauer and Logsdon, 2002).

These statements define the general context in which our study takes place. The main objectives are (i) to assess the effect of rock fragments on the hydraulic conductivity of soil and (ii) to test the validity of the aforementioned models.

2 Material and methods

We performed evaporation experiments and constant-head permeameter tests to study the effect of R_v on saturated and unsaturated hydraulic conductivity by means of laboratory and numerical experiments involving different amounts and types of coarse fragments. We also completed numerical permeability experiments in order to further investigate the effect of the stones' size and shape on the K_se.

2.1 Models predicting soil hydraulic properties of stony soils

Multiple equations have been proposed to estimate the effective saturated hydraulic conductivity of stony soil (K_{se}) from the one of the fine earth (K_s) assuming that rock fragments only decrease the volume available for water flow. The relative saturated hydraulic conductivity (K_r) is defined as the ratio between the K_{se} and the K_s. Equations (1) and (2) have been derived by Peck and Watson (1979) based on heat transfer theory for a homogeneous medium containing non-porous spherical and cylindrical inclusions, respectively. Assuming that stones are non-porous and do not alter the porosity of the fine earth, Ravina and Magier (1984) approximated the K_r to the volumetric percentage of fine earth (Eq. 3). According to empirical relations, Brakensiek et al. (1986) proposed a similar equation, but involving the mass fraction of the rock fragments instead of the volumetric fraction (Eq. 4). On the basis of numerical simulations, Novák et al. (2011) proposed to describe the K_{se} of stony soils as a linear function of the R_v and a parameter that incorporates the hydraulic resistance of the stony fraction (Eq. 5).

$$K_r = \frac{2(1-R_v)}{2+R_v} \qquad \text{Peck and Watson for spherical stones (1979)} \tag{1}$$

$$K_r = \frac{(1-R_v)}{1+R_v} \qquad \text{Peck and Watson for cylindrical stones (1979)} \tag{2}$$

$$K_r = (1-R_v) \qquad \text{Ravina and Magier (1984)} \tag{3}$$

$$K_r = (1-R_w) \qquad \text{Brakensiek et al. (1986)} \tag{4}$$

$$K_r = (1-aR_v) \qquad \text{Novák et al. (2011)} \tag{5}$$

In which R_v is the volumetric stoniness [$\mathrm{L^3\,L^{-3}}$]; R_w is the mass fraction of the rock fragment (mass of stones divided by the total mass of the soil containing stones; the stone density is typically 2.5 $\mathrm{g\,cm^{-3}}$ in this case) [$\mathrm{M\,M^{-1}}$]; a is an empirical parameter that incorporates the hydraulic resistance of the stony fraction (the recommended value is 1.32 for clay soils according to Novák et al., 2011).

Two major characteristics are widely used to describe the hydraulic properties of water in the soil: the water retention curve $\theta(h)$ and the hydraulic conductivity curve $K(h)$. These are both non-linear functions of the pressure head h. One of the most commonly used analytical models has been introduced by van Genuchten (1980), based on the pore size distribution of Mualem (1976), and given by:

$$S_e(h) = \frac{\theta(h) - \theta_r}{\theta_s - \theta_r} = \begin{cases} \left(1 + |\alpha h|^n\right)^{-m} \text{ if } h < 0 \\ 1 \text{ if } h \geq 0 \end{cases} \tag{6}$$

$$K(S_e) = \begin{cases} K_s S_e^l \left[1 - (1 - S_e^{1/m})^m\right]^2 \text{ if } h < 0 \\ K(S_e) = K_s \text{ if } h \geq 0 \end{cases} \tag{7}$$

In which h is the pressure head [L]; $S_e(h)$ is the saturation state [$\mathrm{L^3\,L^{-3}}$]; $\theta(h)$ is the volumetric water content [$\mathrm{L^3\,L^{-3}}$]; θ_r and θ_s respectively represent the residual and saturated water content [$\mathrm{L^3\,L^{-3}}$]; K_s is the saturated hydraulic conductivity [$\mathrm{L\,T^{-1}}$]; n [–], l [–], α [$\mathrm{L^{-1}}$] are empirical shape parameters ($m = 1 - 1/n, n > 1$). If the shape parameters of the van Genuchten/Mualem (VGM) equations (α, n and l) would be independent of R_v (Hlaváčiková and Novák, 2014), one could extend the hydraulic conductivity curves to stony soils using one of the models for K_{se} introduced earlier (Eqs. 1 to 5).

2.2 Laboratory experiments

2.2.1 Sample preparation

We performed laboratory experiments on disturbed samples containing a mixture of fine earth and coarse inclusions. Two types of inclusions were used: rock fragments with a mean diameter between 1 and 2 cm (1) and spherical glass spheres with a diameter of 1 cm (2). The fine earth is classified as a clay (sand: 26 %, silt: 19 %, clay: 55 %).

Before each measurement campaign, fine earth was first oven dried for 24 h at 105 °C and passed through a 2-mm sieve. To prepare a sample without any inclusion, fine earth was compacted layer-by-layer to get an overall bulk density of 1.51 $\mathrm{g\,cm^{-3}}$ (equal to the mean bulk density of the fine earth in situ). For samples containing rock fragments, stones were divided into 4 layers and laid on the fine earth bed on their flattest side. The samples were then compacted in a way that maintains the same bulk density of fine earth. A similar method was applied to samples containing glass balls and rock fragments. Once the specimen was made, it was placed during at least 24 h in a basket containing a thin layer of water in order to saturate the soil from below.

2.2.2 Unsaturated hydraulic conductivity

Setup description

We used the evaporation method to determine the hydraulic conductivity and the retention curve of a soil sample. The principle of this method is to simultaneously measure the matric head at different depths and the water content of an initially saturated soil sample submitted to evaporation.

The experiments were performed over cylindrical Plexiglas samples of 1 L (height: 65 mm), perforated at the bottom to allow saturation from below and open to atmosphere on the upper side to allow evaporation of the soil moisture. Four 6 mm-long ceramic tensiometers (SDEC230) were introduced at 10, 25, 40 and 55 mm in height, respectively denoted T1 to T4 (the reference level is located at the bottom of the sample). In order to avoid preferential flow due to the introduction of the tensiometers on a same vertical line, each hole of the sample was horizontally shifted of 12 degrees vis-à-vis the center of the tube. The tensiometers are connected through a tube to a pressure transducer (DPT-100, DELTRAN). The setup was filled with degased water. The variation in pressure of the drying soil was recorded every 15 min by a CR800 (CAMPBELL SCIENTIFIC). Tensions beyond the consolidation point were not taken into account. The consolidation point refers to the state from which the measured pressure head starts to decrease as bubbles appear and water vapour accumulates (typically 68 kPa cm in this case).

The total water loss as a function of time was monitored by a balance (OHAUS) with a sensitivity of 0.2 g with an accuracy of ±1 g with a time resolution of 15 min. A 50 W infrared lamp was positioned 1 m above the sample surface to slightly speed up the evaporation process. The light was turned off for the first 24 h of every experiment, as the evaporation rate is already high in a saturated sample. A measuring campaign lasted until 3 of the 4 tensiometers ran dry (the tension sharply drops down to approximately a null value). At the end of the experiment, the sample was oven dried for 24 h at 105 °C to estimate the θ.

Data processing

A simplified Wind's method (1968) was used to transform matric potential and total weight data over time into the hydraulic conductivity curve (Schindler, 1980, cited by Schindler and Müller, 2006; Schindler et al., 2010). The method is further adapted in order to take into account the data from 4 tensiometers (data points for the hydraulic conductivity curve is made for every possible combination of two tensiometers). The method assumes that the distribution of water tension and water content is linear through the soil column. It further linearizes the water tension and the mass changes over time. The time step chosen to process the data is one hour.

The water retention curve $\theta(h)$ is calculated using the mean tension and the weight measurements from the scale (for information purposes only). A first step to determine the hydraulic conductivity curve $K(h)$ is to calculate the rate of water flow q through the cross-section in between tensiometers j and k at time t^i, which is calculated as follows:

$$q^i_{jk} = \frac{z_j + z_k}{2L}\left(\frac{-\Delta M^i}{\Delta t^i \rho_\mathrm{w} A}\right) \tag{8}$$

In which q is the cross-sectional water flow [L T^{-1}]; z_j and z_k respectively represent the height of tensiometer j and k [L] (the reference level is located at the bottom of the sample); L is the height of the tube [L]; ΔM^i is the mass difference measured by the scale [M]; $\Delta t^i = t^i - t^{i-1}$ is the time interval [T]; ρ_w is the density of water [M L^{-3}] and A is the cross-section of the tube [L^2].

Afterwards, the hydraulic conductivity K at time t^i can be deduced from measurement in tensiometer j and k inverting the Darcy equation:

$$K^i_{jk} = \frac{q^i_{jk}}{\Delta h^i_{jk}/\Delta z_{jk} - 1} \tag{9}$$

In which K is the hydraulic conductivity [L T^{-1}]; $\Delta z_{jk} = z_k - z_j$ is the height difference between tensiometer z and j [L] and Δh^i_{jk} is the mean difference of water tension between tensiometer z and j in the middle of the time interval defined by t^{i-1} and t^i [L]:

$$\Delta h^i_{jk} = \frac{(h^{i-1}_k - h^{i-1}_j) + (h^i_k - h^i_j)}{2} \tag{10}$$

The mean matric head corresponding to the two tensiometers used to evaluate conductivity is calculated as follows:

$$h^{\bar{i}}_{jk} = \frac{h^{i-1}_k + h^{i-1}_j + h^i_k + h^i_j}{4} \tag{11}$$

By calculating the hydraulic conductivity based on measurement of tensiometers j and k and linking it to the corresponding mean matric head, one can thus evaluate the point of the hydraulic conductivity curve $K^i_{jk}(h^{\bar{i}}_{jk})$. We used every possible combination of 2 tensiometers (6 here) to obtain data points for the hydraulic conductivity curve.

Points of the hydraulic conductivity curve obtained at very small hydraulic gradients were rejected, because large errors occur in the near-saturation zone due to uncertainties in estimating small hydraulic gradients (Peters and Durner, 2008; Wendroth, 1993). This highlights in its turn the necessity of reliable tensiometers to estimate the near-saturated hydraulic conductivity. In the current literature, acceptation limits of the hydraulic gradient vary between 5 and $0.2\,\mathrm{cm\,cm^{-1}}$ (Mohrath et al., 1997; Peters and Durner, 2008; Wendroth, 1993). Using the least restrictive filter criterion (hydraulic gradient > 0.2) requires fine calibration and outstanding performance of the tensiometers. Choosing a more restrictive criterion leads to a larger loss of conductivity points, but provides more reliable and robust data. We decided to use a filter criterion that does not consider hydraulic conductivity points higher than the evaporation rate (from 0.1 to $0.2\,\mathrm{cm\,day^{-1}}$ in this case), resulting in a lower limit of $1\,\mathrm{cm\,cm^{-1}}$ for the hydraulic gradient.

As pointed out by Wendroth (1993) and Peters and Durner (2008), the main drawback associated with the evaporation experiment is that no estimates of conductivity in the wet range can be obtained due to the typically small hydraulic gradients so that additional measurements of the K_{se} should be provided. To do so, we used constant-head infiltration permeameter tests (see below).

Except for the K_{se} which is fixed using results from the constant-head permeameter tests, the parameters of the VGM-model (1980) (Eq. 7) are obtained by fitting evaluation points from each combination of tensiometers using the so-called “integral method” (Peters and Durner, 2006).

2.2.3 Saturated hydraulic conductivity

Constant-head permeability tests were used to determine the K_{se} of saturated cylindrical core samples. The flow through the sample is measured at a steady rate under a constant pressure difference. The K_{se} can thus be derived using the following equation:

$$K_{se} = \frac{VL}{A\Delta H \Delta t} \tag{12}$$

In which V is the volume of discharge [L^3]; L is the length of the permeameter tube [L]; A is the cross-sectional area of the permeameter [L^2]; ΔH is the hydraulic head difference across the length L [L] and Δt is the time for discharge [T].

The soil sample, the same size as the one from the evaporation experiment, was extended on its upper side by a paper tape. A 2 cm thick layer of water was maintained on top of the sample thanks to a water reservoir with a beveled outlet. Water was collected through a funnel in a burette and the volume of discharge V was deduced from measurements after 30 and 210 min after the beginning of the experiment (Δt = 180 min).

2.3 Numerical experiments

HYDRUS-2D software was used to simulate water flow in variably saturated porous stony soils. HYDRUS-2D is a two-dimensional finite element model based on Richard's equation.

All the performed simulations assumed that rock fragments were non-porous so that "no-flux" boundaries conditions were specified along the stones limits. Rock fragments were supposed to be circular. The soil domain over which simulations were performed had the same dimensions as the longitudinal section of the sampling ring used in the laboratory experiments (14 × 6.5 cm). The parameters of fine earth used in the simulations were obtained by inversion using the hydraulic conductivity and water retention curves obtained in our laboratory experiments on stone-free samples (Table 1).

2.3.1 Unsaturated hydraulic conductivity

We repeated the evaporation test as virtual experiment. The top boundary of the virtual sample was submitted to an evaporation rate q of 0.1 cm day^{-1} during 14 days. No fluxes were allowed across other boundaries.

The calculation method applied to the output data was similar to the laboratory evaporation experiment, except that the conductivity and pressure head estimations resulted from 2 observation nodes placed at the top and the bottom of the profile (the pressure head was linearly distributed across the soil profile).

As numerical errors occur in the near-saturation zone of the virtual evaporation experiment, extra simulations were required to minimize the extrapolation error of the hydraulic conductivity curve from the evaporation experiment data to the near-saturation zone. Although the causes are different, both real and virtual experiments require the addition of data from permeameter tests. As for the laboratory experiment, the hydraulic conductivity curve was obtained fitting the discrete conductivity data using the so-called "integral method" (Peters and Durner, 2006).

2.3.2 Saturated hydraulic conductivity

The K_{se} was determined using a numerical constant-head permeability test. We simulated a steady-state water flow of a saturated soil profile, with a constant head of 10 cm applied on the upper boundary. The bottom boundary of the column was defined as a "seepage face", which means that water starts flowing out as soon as the soil at the boundary reaches saturation. The calculation method applied to the output data was identical to the laboratory constant head permeameter.

2.4 Treatments

Table 2 presents a scheme of all the performed experiments. We first studied the effect of R_v on unsaturated hydraulic properties using laboratory and numerical experiments.

In the laboratory approach, we performed evaporation experiments on samples containing (i) fine earth only and (ii) on others with rock fragments (1) at a R_v of 20 %. Two replications per treatment were performed (4 measurement campaigns in total). For the numerical approach, simulations of the evaporation experiment were done on homogeneous soil (without stones) and on soil with a R_v of 10, 20 and 30 %. Having less time-constraints in the virtual experiment, we added an increasing R_v to observe the evolution of the hydraulic conductivity curve. Simulations were performed on soil samples containing 12 regularly distributed stones. The accuracy of the conductivity curve from the evaporation experiment in the near-saturated zone was improved by using real and virtual permeameter tests. One can notice that no investigations of the unsaturated properties with coarse fragments above 30 % of R_v were performed. Indeed, given that small variations of the hydraulic gradient can lead to substantial changes in the hydraulic conductivity estimates, the tensiometers should be ideally positioned out of the direct influence of one particular stone in order to obtain generalizable results. This implies the need for relatively low stone contents ($<$ 30 % according to Zimmerman and Bodvarsson, 1995).

Then, to study the relationship between K_{se} and R_v, we tested 2 types of inclusions (rock fragments (1) and glass spheres (2)) and 4 volumetric fractions (0, 20, 40 and 60 %). We did not perform any replications since the setup was totally artificially controlled. The only source of uncertainty is the homogeneous compaction of the fine earth fraction. Virtual permeameter tests were also performed involving 12 circular regularly distributed inclusions for the same R_v (0, 20, 40, 60 %).

In addition, we used the virtual permeameter experiment to investigate the effect of the inclusion shape and size on K_{se}. To do so, simulations of the permeameter test were performed on soil containing stones of 5 different shapes: circular, upward equilateral triangle, downward equilateral triangle, rectangle on its shortest side (L × 1.5 L) and rectangle on its longest side (1.5 L × L) with an R_v of 10, 20 and 30 %. We first performed simulations on soil containing only one centered inclusion. We also performed permeameter tests on soil containing 12 and 27 regularly distributed inclusions (for each R_v).

3 Results and discussion

In the following, results from real and virtual experiments will be compared to the predictions of the different models developed in Sect. 2.1. The K_{se} will be represented by the median value predicted by the 5 models linking the properties of fine earth to the ones of stony soil (Eqs. 1 to 5). The same models assume that the shape parameters of the VGM-equations, n, l and α, do not depend of the stoniness. This will be referred to as "results from the models" in the following and will be graphically represented by dotted lines.

3.1 Effect of stones on saturated hydraulic conductivity

Figure 1 shows the relationship between the relative saturated hydraulic conductivity (K_r) and the volumetric stone content (R_v) obtained from the constant-head permeability tests for laboratory and numerical experiments. The figure also depticts the median K_r of the models (dashed line) and the error bars show its 95 % confidence intervals.

The models predict a decreasing K_{se} for an increasing R_v. Numerical experiments also simulate a decrease in K_{se} with an increasing R_v similar to the models. Regarding the real experiments with samples containing rock fragments, we can observe that the measured K_{se} decreases in the same way as the models until a R_v of 20 %. For higher R_v, the tendency is reversed and K_{se} begins to increase. This decreasing then increasing relationship with an increasing R_v supports the results of Beibei et al. (2009) and Ma et al. (2010). Other factors than the reduction of the volume available for water flow have therefore a significant effect on K_{se}. We hypothesize that, from a certain R_v onward, voids at the stone-fine earth interface create a more continuous macropore system that overcomes the other drivers reducing the effective K. This formation of macropores between the rock fragment surface and the fine earth fraction has already been pointed out by Beibei et al. (2009), Ravina and Magier (1984) and Sauer and Logsdon (2002) to explain results obtained in similar experiments.

Ravina and Magier (1984) mention that compaction of a saturated sample creates voids near the stone surface and hence increases K_{se} with an increasing R_v. Our experiments show a similar behavior for dry soils (the disturbed samples were build compacting dry fine earth). As soil compaction often occurs naturally in the field (especially through consolidation processes), its effect should not be neglected.

We observed the same complex behavior during the experiment with glass balls. Moreover, we observed a nearly linear upward trend directly from the beginning. The large variation between the trends of the two curves suggests that K_{se} also depends on the shape and the roughness of the inclusions. We hypothesize that the roughness of the inclusions could alter the K_{se} by changing the amount and the type of voids in the stone vicinity. Nevertheless, we can only see the combined effect of these two factors – roughness and shape – in this experiment.

These considerations suggest that the relationship between K_{se} and R_v proposed by the models simplifies reality to a great extent. However, the understanding of the major drivers of the K_{se} and their relative importance remains unclear. The effect of the size and shape of stones as such can be explored through simulations, but the void effect is less easy to determine. A solution to this problem could be the use of imaging techniques such as X-ray CT to observe the structure of the fine earth fraction.

3.2 Effect of the stones' size and shape on the saturated hydraulic conductivity

To investigate the effect of the size of the inclusions and their shape on K_{se}, we performed virtual constant-head permeameter experiments on samples containing 1, 12 and 27 inclusions of various shapes, for a R_v of 10, 20 and 30 %. Figures 2 to 4 illustrate the tendency of the effects and their respective drivers. The complete set of results can be found in Table A1 in the Appendix.

Figure 2 represents the K_r for different sizes of circular inclusions and increasing overall stone content (R_v). When the size of the inclusions decreases (when the number of inclusions increases for a same R_v), the K_r tends to decrease. An interaction between the R_v and the size of inclusion can be observed: the effect of size is more marked with a higher R_v. For example, the decrease in K_r between 1 and 27 circular inclusions is limited to 2 % for a R_v of 10 %, but rises up to 25 % for a R_v of 30%. A similar behavior is observed with simulations for different shapes of inclusions. These statements support the findings of Novák et al. (2011): the smaller the stones, the higher the resistance to flow at a given stoniness. We suggest the decrease of K_{se} is due to a combination of the two following phenomena. The first one is the overlapping of the influence zone of each inclusion, causing further reduction of K_r. The concept of overlapping influence zones was first proposed by Peck and Watson (1979) to explain higher decrease of the hydraulic conductivity of stones very close to each other in comparison to isotropically distributed stones. The second phenomenon could be that, for a given R_v, the contact area between stones and fine earth is higher for small stones than for bigger ones. Hence, a higher tortuosity can be responsible for a lower flow rate.

The shape of the inclusions has also a significant impact on K_r. Figure 3 shows the K_r as a function of R_v for different inclusion shapes in a profile containing 12 inclusions. For a fixed number of inclusions, the K_r is higher with rectangular inclusions on their shortest side and smaller with rectangular inclusions on their longest side. Circular inclusions provoke a smaller reduction than triangular inclusions. The orientation of the triangles does not have a pronounced effect on K_r. Here again, we observe a stronger effect of the size for higher stoniness. As an illustration, the decrease in K_r between circular and triangular inclusions is limited to 5 % for a R_v of 10 % but rises up to 14 % for a R_v of 30 %. A similar behavior is observed with simulations including either 1 or 27 fragments.

Figure 4 displays the K_r for different inclusions shape and size, for a fixed R_v of 20 %. The effect of the shape of the inclusions depends on their size. E.g., the decrease in K_r between rectangular inclusions positioned on their longest and shortest sides is limited to 13 % for samples containing one inclusion only while it is as high as 21 % for samples containing 27 inclusions. Inversely, the effect of the size of inclusions also depends on their shape. This effect is higher for triangular and rectangular inclusions positioned on their longest side, with a K_r decrease between 1 and 27 inclusions of 23 and 18 % respectively. This effect is less significant for circular inclusions and for rectangular inclusions positioned on their shortest sides. The associated K_r decrease between 1 and 27 inclusions is 11 and 10 % respectively.

The median value of K_r predicted by the models for a R_v of 20 % (0.73) is similar to the K_r measured on samples containing only one spherical inclusion (Fig. 4). The K_r predicted by the models is always higher than the K_r determined by the simulations, except for soils containing one inclusion on its shortest side. One can conclude that the shape and the size of inclusions have a significant effect on K_{se}, which is usually neglected by the models.

3.3 Effect of stones on unsaturated hydraulic conductivity

Figure 5 represents the hydraulic conductivity curves obtained from the virtual permeameter and evaporation experiments for different stoniness (R_v = 0, 10, 20 and 30 %) as well as results predicted by the models for the corresponding R_v. The hydraulic conductivity curves from the models and from the numerical experiments match hydraulic conductivity decreases for increasing R_v. According to these experiments, hydraulic conductivity in the unsaturated zone is well defined using a correct K_{se} and shape parameters do not dependent on the stoniness.

We have to keep in mind that both the models and the numerical experiments cannot simulate other possible impacts of stones like the creation of voids at the inclusion vicinity unless we create them manually in the domain. They also both assume that stones are non-porous. This explains the close concordance of results from models and numerical experiments.

Figure 6 represents the hydraulic conductivity curves obtained from laboratory experiments on stone-free samples and on samples with a R_v of 20 % as well as the results predicted by the models for a R_v of 20 %. Even though the data points are dispersed, those coming from the evaporation experiments measured on stony samples are globally lower and slightly more flattened than the ones measured on stone-free samples. This suggests that stones decrease hydraulic conductivity, whatever the suction may be.

The hydraulic conductivity curve predicted by the models is higher than the fitted hydraulic conductivity curve from the evaporation experiments on the stony samples. This is linked to the fact that the fitted curve has been "forced" by the additional K_{se} data point at zero tension. The K_{se} predicted by the models is 1.95 cm day^{-1} while the K_{se} measured with the permeameter is 1.55 cm day^{-1}. We can explain such a difference (20 %) in K_{se} by the way stones are positioned in the sample: stones were laid on their flattest side for practical reasons. As confirmed by the numerical simulations, they could therefore have hampered the water flow more strongly than if they were positioned differently.

In the numerical experiments, the presence of stones reduced the hydraulic conductivity in the same way as predicted by the models, whatever the suction was. Similarly, the laboratory experiments suggested that stones reduce the hydraulic conductivity at high suction (pF > 2). Nevertheless, laboratory experiments in saturated conditions indicated that voids creation at the stone-fine earth interface might increase the K_{se}. According to the well-know law of Jurin (1717), pores through which water will flow depend both on the pore size distribution and the effective saturation state. The flow in the macropore system will be only "activated" in the near-saturation zone while small pores will be only drained at high suction. Therefore, we can hypothesize that even if it is not clear whether stones increase or decrease the near-saturation hydraulic conductivity, they are always expected to decrease the hydraulic conductivity at low effective saturation states. As a total saturation of the soil is rarely reached in practice (Gras, 1994), considering a diminishing hydraulic conductivity with an increasing R_v seems appropriate. However, under saturated conditions, the macropores have a non-negligible effect so that understanding the relationship between R_v and K_se requires further investigations.

4 Conclusion

Determining the effect of rock fragments on soil hydraulic properties is a major issue in soil physics and in the study of fluxes in soil-plant-atmosphere systems in general. Several models aim at linking the hydraulic properties of fine earth to those of stony soil. Many of them assume that the only effect of stones is to reduce the volume available for water flow. We tested the validity of such models with various complementary experiments.

Our results suggest that considering that stones only reduce the volume available for water flow many be ill-founded. We pointed out several other drivers influencing K_se which are not considered by these models. We observed that, for a given stoniness, the resistance to flow is higher for smaller inclusions than for bigger ones. We explain this tendency by an overlapping of the influence zones of each stone combined with a higher tortuosity of the flow path. We also pointed out the shape of stones as a major factor affecting the hydraulic conductivity of the soil. We showed that the effect of the shape depends on the inclusion size and inversely that the effect of inclusion size depends on its shape. Finally, we proposed that soil compaction, swelling and shrinking might strongly alter the K_se via the creation of voids at the stone-fine earth interface as pointed out by Ravina and Magier (1984). Even if the very mechanisms behind the creation of voids remains unclear, its effect seems to strongly depend on the R_v, the shape and the roughness of inclusions. We also hypothesize that the fine earth texture plays a major role in the voids creation.

These findings suggest the aforementioned models are not appropriate in all cases, particularly under saturated conditions. However, under unsaturated conditions, this statement should be more nuanced, as both numerical and laboratory experiments corroborate the general trends from the models. Models should at least take into account the effect of the size and the shape of stones as well as the voids creation induced by stones. However, the mechanisms governing the creation of voids at the stone-fine earth interface still need to be explored.

Further investigations are thus required in order to explore the hydraulic properties of stony soils and to define the conditions under which we can apply the models. The direct observation of undisturbed stony samples porosity using X-ray computed tomography or magnetic resonance imaging is a necessary next step to a better understanding of the link between void creation at the stone-fine earth interface and soil compaction. Finally, similar analyses should be conducted in view of determining the effect of the fine earth texture on the drivers of hydraulic properties as pointed out throughout our research.

Acknowledgements. We thank Stephane Becquevort of the soil physics lab for his support in setting up the experiments. The laboratory measurements of this study will be available upon publication of the paper at doi:10.5281/zenodo.32661.

References

Beibei, Z., Ming'an, S., and Hongbo, S.: Effects of rock fragments on water movement and solute transport in a Loess Plateau soil, Comptes Rendus Geosci., 341, 462–472, 2009.

Bouwer, H. and Rice, R. C.: Hydraulic Properties of Stony Vadose Zones, Ground Water, 22, 696–705, 1984.

Brakensiek, D. L., Rawls, W. J., and Stephenson, G. R.: Determining the Saturated Hydraulic Conductivity of a Soil Containing Rock Fragments1, Soil Sci. Soc. Am. J., 50, 834–835, doi:10.2136/sssaj1986.03615995005000030053x, 1986.

Buchter, B., Hinz, C., and Flühler, H.: Sample size for determination of coarse fragment content in a stony soil, Geoderma, 63, 265–275, 1994.

Cousin, I., Nicoullaud, B., and Coutadeur, C.: Influence of rock fragments on the water retention and water percolation in a calcareous soil, Catena, 53, 97–114, 2003.

García-Ruiz, J. M.: The effects of land uses on soil erosion in Spain: A review, Catena, 81, 1–11, 2010.

Gusev, Y. and Novák, V.: Soil water – main water resources for terrestrial ecosystems of the biosphere, J. Hydrol. Hydromech. Slovak Repub., 55, 3–15, 2007.

Hlaváčiková, H. and Novák, V.: A relatively simple scaling method for describing the unsaturated hydraulic functions of stony soils, J. Plant Nutr. Soil Sci., 177, 560–565, 2014.

Jurin, J.: An Account of Some Experiments Shown before the Royal Society; With an Enquiry into the Cause of the Ascent and Suspension of Water in Capillary Tubes, Philos. Trans., 30, 739–747, 1717.

Ma, D. and Shao, M.: Simulating infiltration into stony soils with a dual-porosity model, Eur. J. Soil Sci., 59, 950–959, 2008.

Ma, D., Zhang, J., Ma, D., Shao, M., Wang, Q., and Ma, D.: Validation of an analytical method for determining soil hydraulic properties of stony soils using experimental data, Geoderma, 159, 262–269, 2010.

Miller, F. T. and Guthrie, R. L.: Classification and distribution of soils containing rock fragments in the United States, Eros. Product, Soils Contain. Rock Fragm. SSSA Spec Publ., 13, 1–6, 1984.

Mohrath, D., Bruckler, L., Bertuzzi, P., Gaudu, J. C., and Bourlet, M.: Error Analysis of an Evaporation Method for Determining Hydrodynamic Properties in Unsaturated Soil, Soil Sci. Soc. Am. J., 61, 725–735, 1997.

Novák, V. and Kňava, K.: The influence of stoniness and canopy properties on soil water content distribution: simulation of water movement in forest stony soil, Eur. J. For. Res., 131, 1–9, 2011.

Novák, V. and Šurda, P.: The water retention of a granite rock fragments in High Tatras stony soils, J. Hydrol. Hydromech., 58, 181–187, 2010.

Novák, V., Kňava, K., and Šimůnek, J.: Determining the influence of stones on hydraulic conductivity of saturated soils using numerical method, Geoderma, 161, 177–181, 2011.

Peck, A. J. and Watson, J. D.: Hydraulic conductivity and flow in non-uniform soil, Workshop on Soil Physics and Soil Heterogeneity, CSIRO Division of Environmental Mechanics, Canberra, Australia, 1979.

Peters, A. and Durner, W.: Improved estimation of soil water retention characteristics from hydrostatic column experiments, Water Resour. Res., 42, W11401, doi:10.1029/2006WR004952, 2006.

Peters, A. and Durner, W.: Simplified evaporation method for determining soil hydraulic properties, J. Hydrol., 356, 147–162, 2008.

Poesen, J. and Lavee, H.: Rock fragments in top soils: significance and processes, CATENA, 23, 1–28, 1994.

Ravina, I. and Magier, J.: Hydraulic Conductivity and Water Retention of Clay Soils Containing Coarse Fragments, Soil Sci. Soc. Am. J., 48, 736–740, 1984.

Russo, D.: Leaching Characteristics of a Stony Desert Soil1, Soil Sci. Soc. Am. J., 47, 431–438, 1983.

Sauer, T. J. and Logsdon, S. D.: Hydraulic and physical properties of stony soils in a small watershed, Soil Sci. Soc. Am. J., 66, 1947–1956, doi:10.2136/sssaj2002.1947, 2002.

Schindler, U.: Ein Schnellverfahren zur Messung der Wasserleitfähigkeit im teilgesättigten Boden an Stechzylinderproben, Arch. Acker. Pfl. Boden., 24, 1–7, 1980.

Schindler, U. and Müller, L.: Simplifying the evaporation method for quantifying soil hydraulic properties, J. Plant Nutr. Soil Sci., 169, 623–629, 2006.

Schindler, U., Durner, W., von Unold, G., and Müller, L.: Evaporation Method for Measuring Unsaturated Hydraulic Properties of Soils: Extending the Measurement Range, Soil Sci. Soc. Am. J., 74, 1071, doi:10.2136/sssaj2008.0358, 2010.

van Genuchten, M. T.: A Closed-form Equation for Predicting the Hydraulic Conductivity of Unsaturated Soils, Soil Sci. Soc. Am. J., 44, 892–898, 1980.

Wendroth, E.: Reevaluation of the evaporation method for determining hydraulic functions in unsaturated soils, Soil Sci. Soc. Am. J., 57, 1436–1443, 1993.

Wind, G. P.: Capillary conductivity data estimated by a simple method, 181–191, in: Water in the unsaturated zone, Proc. Wageningen Symp., the Netherlands, 19–25 June 1966, Vol. 1. Publ. 82, edited by: Rijtema, P. P. E. and Wassink, H., Int. Assoc. Scientific Hydrol., Gentbrugge, Belgium, 1968.

Zimmerman, R. W. and Bodvarsson, G. S.: The effect of rock fragments on the hydraulic properties of soils, Lawrence Berkeley Lab., CA, USA, Funding organisation: USDOE, Washington, D.C., USA, 1995.

Title Page
Abstract Introduction
Conclusions References
Tables Figures
◄ ►
Back Close
Full Screen / Esc
Printer-friendly Version
Interactive Discussion

Table 1. Parameters of the van Genuchten equations used in the numerical experiments.

θ_r [–]	θ_s [–]	α [cm^{-1}]	n [–]	l [–]	K_{se} [cm day^{-1}]
0.185	0.442	0.0064	2.11	−0.135	2.686

Table 2. Schematic summary of the treatments (H = Rectangle on its shortest side, O = Circle, ∧ = Upward triangle, v = Downward triangle, L = Rectangle on its longest side).

	Effect of R_v on unsaturated hydraulic conductivity		Effect of R_v on saturated hydraulic conductivity			Effect of size and shape on saturated hydraulic conductivity				
Method	Evaporation experiment + Permeameter		Permeameter			Permeameter				
R_v [%]	0–10–20–30	0–20	0–20–40–60			0–10–20–30				
Approach	Numerical	Laboratory	Numerical	Laboratory		Numerical				
Inclusion type	O (2-D) $n = 12$	Rock fragments	O (2-D) $n = 12$	Glass spheres	Rock fragments	O (2-D) $n = 1$, 12, 27	∧ (2-D) $n = 1$, 12, 27	v (2-D) $n = 1$, 12, 27	H (2-D) $n = 1$, 12, 27	L (2-D) $n = 1$, 12, 27

Table A1. Results from the investigation of the inclusion size and shape on the saturated hydraulic conductivity by means of numerical simulations (*n* is the number of inclusions simulated in the profile for the corresponding R_v, H = Rectangle on its shortest side, O = Circle, ∧ = Upward triangle, v = Downward triangle, L = Rectangle on its longest side).

R_v	Shape	Relative saturated hydraulic conductivity		
		$n = 1$	$n = 12$	$n = 27$
10 %	H	0.88	0.88	0.88
	O	0.84	0.83	0.82
	∧	0.80	0.79	0.78
	v	0.80	0.79	0.78
	L	0.84	0.83	0.82
20 %	H	0.76	0.71	0.68
	O	0.73	0.69	0.65
	∧	0.67	0.63	0.54
	v	0.67	0.63	0.54
	L	0.66	0.61	0.54
30 %	H	0.70	0.60	0.55
	O	0.64	0.58	0.48
	∧	0.59	0.50	0.46
	v	0.59	0.50	0.47
	L	0.56	0.48	0.31

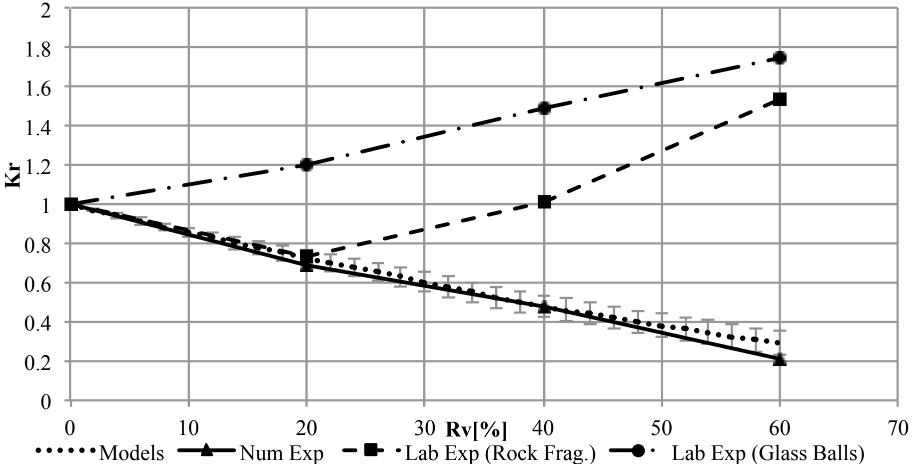

Figure 1. K_{se} depending on R_v obtained from laboratory experiments, numerical experiments and the models (the error bars show the 95 % confidence intervals of median predicted by these models).

Title Page
Abstract Introduction
Conclusions References
Tables Figures
◄ ►
Back Close
Full Screen / Esc
Printer-friendly Version
Interactive Discussion

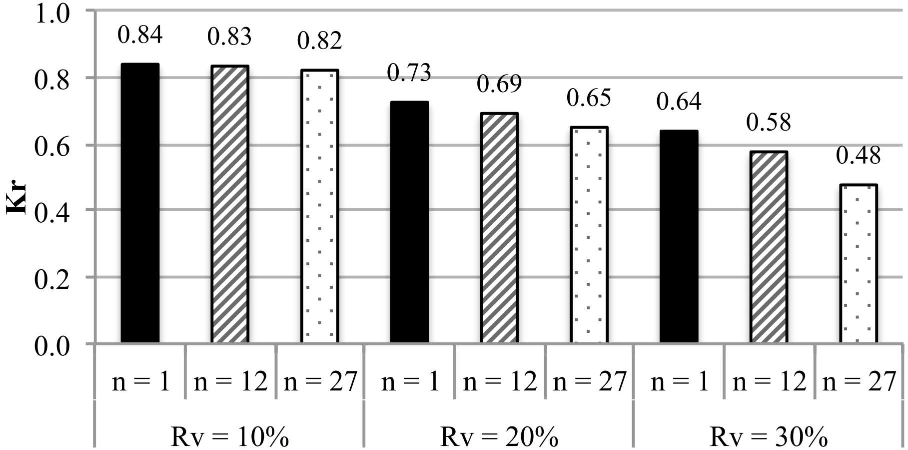

Figure 2. K_r depending on R_v for different sizes of circular inclusions (*n* is the number of inclusions simulated in the profile for the corresponding R_v).

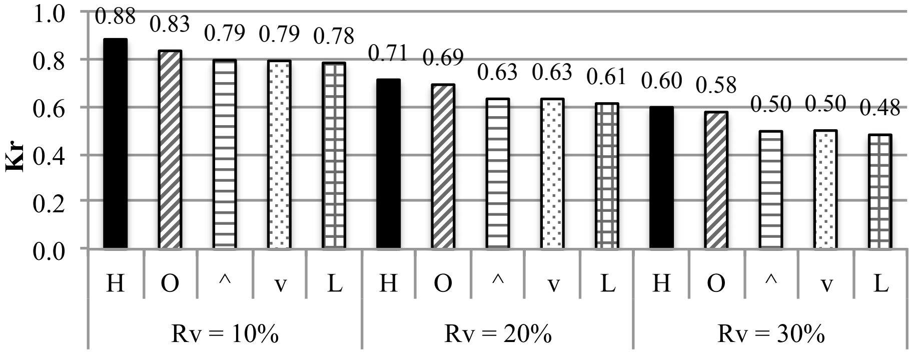

Figure 3. K_r depending on R_v for different inclusion shapes in a profile containing 12 inclusions regularly distributed (H = Rectangle on its shortest side, O = Circle, ∧ = Upward triangle, v = Downward triangle, L = Rectangle on its longest side).

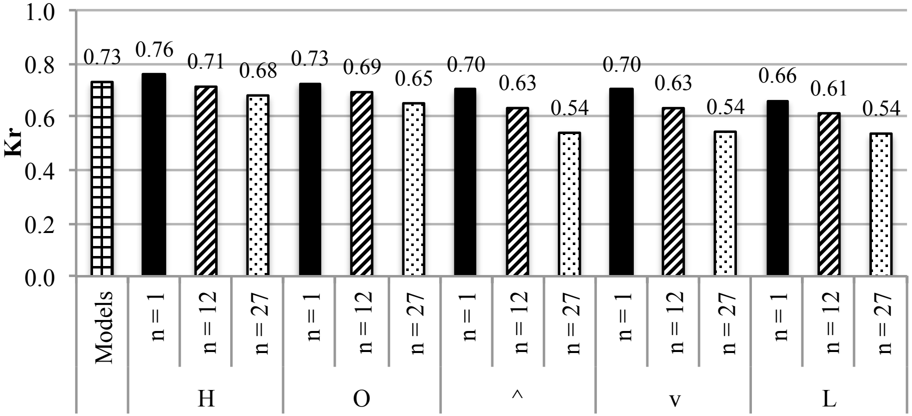

Figure 4. K_r for different inclusion shapes and sizes in a profile with a R_v of 20 % (H = Rectangle on its shortest side, O = Circle, ∧ = Upward triangle, v = Downward triangle, L = Rectangle on its longest side) and median K_r predicted by the models for the corresponding R_v.

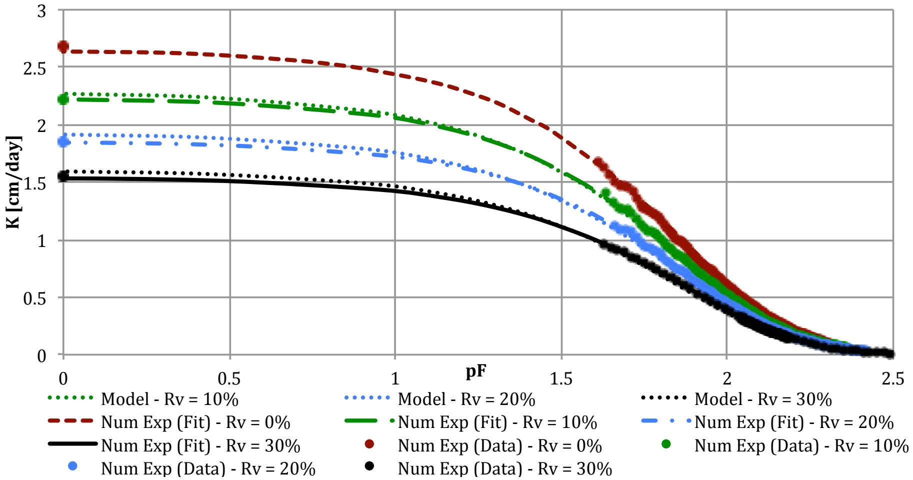

Figure 5. Hydraulic conductivity curves obtained from numerical experiments (data and fit for R_v = 0, 10, 20, 30 %) and results predicted by the models for the coresponding R_v.

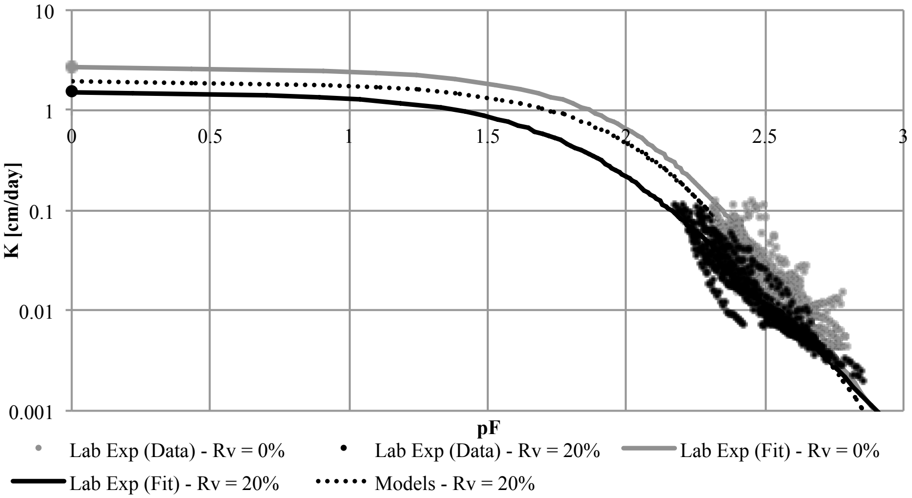

Figure 6. Hydraulic conductivity curves obtained from laboratory experiments (data and fit for R_v = 0 and 20 %) and results predicted by the models for a R_v of 20 %.